

## Signal-background interference in $gg \rightarrow H \rightarrow VV$

---

**Nikolas Kauer\***

*Department of Physics, Royal Holloway, University of London, Egham TW20 0EX, UK*

*E-mail: n.kauer@rhul.ac.uk*

The resonance-continuum interference between the SM Higgs search signal process  $gg \rightarrow H \rightarrow VV$  ( $V = W, Z$ ) and the irreducible background process  $gg \rightarrow VV$  is studied at leading order for integrated cross sections and differential distributions in  $pp$  collisions at  $\sqrt{s} = 7$  TeV and 14 TeV for  $M_H = 400$  GeV. Leptonic weak boson decays are included, and realistic experimental selection cuts are applied.

*10th International Symposium on Radiative Corrections (Applications of Quantum Field Theory to Phenomenology)  
September 26-30, 2011  
Mamallapuram, India*

---

\*Speaker.

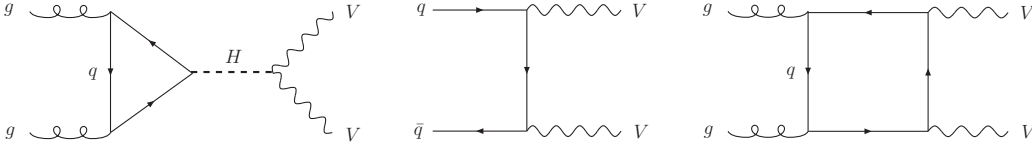


**Figure 1:** Representative Feynman graphs for the Higgs signal process (left) and the  $q\bar{q}$ - (centre) and  $gg$ -initiated (right) continuum background processes at LO.

## 1. Introduction

Higgs production in gluon fusion with subsequent decay into a weak boson pair is an important element of the Higgs search at the LHC. The signal process (Fig. 1, left) has been calculated and studied up to NNLO (see Refs. [1–11] and references therein). Continuum weak boson pair production is the dominant irreducible background and has also been studied extensively. For the leading quark scattering subprocess (Fig. 1, centre), programs at NLO are available, in part based on earlier calculations (see Refs. [12–14] and references therein). Here, we focus on the gluon scattering subprocess (Fig. 1, right) and its interference with the signal process.  $gg \rightarrow VV$  continuum production formally enters at NNLO and was calculated in Refs. [15–18]. Off-shell weak boson decays and the possibility to interface with shower programs were subsequently included [13, 19–25]. At the LHC, the importance of gluon-induced  $VV$  continuum production and decay is enhanced by the large gluon-gluon flux and experimental Higgs search selection cuts. Resonance-continuum interference has been studied for  $gg (\rightarrow H) \rightarrow VV$  in Refs. [11, 16, 17, 22, 24, 26] and for related processes in Refs. [27–29]. Here, results for a heavy Higgs boson with  $M_H = 400$  GeV are presented. The search for a heavy Higgs boson at hadron colliders has been examined in Refs. [30–33].

## 2. Computational details

The results presented in Section 3 have been calculated with the programs gg2WW [20, 22] and gg2ZZ [23]. Representative graphs for the  $gg \rightarrow H \rightarrow VV$  signal process and the  $gg \rightarrow VV$  continuum process are displayed in Fig. 1. In addition to box topologies in principle also triangle topologies contribute to the  $gg$ -initiated continuum processes (see Fig. 2). But, in the limit of vanishing lepton masses the triangle graphs do not contribute.<sup>1</sup> For cross checks, two amplitude codes have been used based on the methods described in Ref. [22] (BCKK) and Refs. [34, 35] (FormCalc). Off-shell weak boson contributions and massless as well as massive quarks are taken into account. Third quark generation contributions increase the total  $gg \rightarrow WW \rightarrow$  leptons continuum cross section by 12% and the double-resonant  $gg \rightarrow ZZ \rightarrow$  leptons continuum cross section by 65% ( $pp$ ,  $\sqrt{s} = 14$  TeV). For  $Z$ -pair production and decay, the  $\gamma^*$  contributions are taken into account. For  $W$ -pair production and decay, the BCKK code approximates  $V_{CKM} = 1$ . The FormCalc code was used to confirm at the amplitude level that this is an excellent approximation as CKM effects

<sup>1</sup>Note that the  $gg \rightarrow Z$  triangle graphs do contribute for non-zero lepton masses, which was verified by explicit calculation.



**Figure 2:** Representative triangle graphs that formally contribute to gluon-induced  $VV$  continuum production and decay.

are smaller than 0.01%. The  $gg2VV$  programs allow for the simultaneous calculation of cross sections for multiple scales as well as the PDF error.<sup>2</sup>

As both amplitude implementations employ Passarino-Veltman-type tensor integral reduction methods, a discussion of numerical stability is warranted. The box amplitudes are affected by spurious singularities, which are caused by inverse powers of the Gram determinant  $\det G = 2s(tu - M_{V_1}^2 M_{V_2}^2)$ , because  $\det G \rightarrow 0$  as  $p_{TV} \rightarrow 0$ . For phenomenologically relevant cross sections, the error caused by numerical instabilities should be small compared to practical MC integration errors, which are typically of order 0.1%. After the symbolic cancellation of Gram determinants, the BCKK amplitude code evaluated in quadruple precision is numerically stable in the above sense.<sup>3</sup> On the other hand, numerical instability is observed for the FormCalc amplitude code when evaluated in quadruple precision for a relevant phase space (PS) configuration with  $p_{TV} = 0.007$  GeV. Using the stable BCKK code as benchmark, the following diagnostic algorithm was devised to detect problematic PS points with the FormCalc code and quadruple precision: First, we exploit that instabilities spoil Lorentz invariance by comparing  $|\mathcal{M}|^2$  evaluated at the PS point and the PS point boosted along the beam axis with  $p_{\text{boost}} = (1, 0, 0, 0.001 + 0.1 r_1)$  GeV with random  $r_1 \in [0, 1]$ .<sup>4</sup> The relative deviation is assessed using  $\text{reldev}(x, y) = |x - y| / \min(x, y)$ . If  $\text{reldev}(|\mathcal{M}|^2, |\mathcal{M}_{\text{boosted}}|^2) > 10^{-4}$  the PS point is classified as unstable. The same criterion is then applied again, except now with a random boost in the opposite direction. If the PS point is still considered stable another test is performed, which exploits that instabilities occur at exceptional PS configurations. One therefore compares  $|\mathcal{M}|^2$  evaluated at the PS point (in double precision) and the PS point mapped to single precision. If  $\text{reldev}(|\mathcal{M}|^2, |\mathcal{M}_{\text{single}}|^2) > 1$  the PS point is classified as unstable. Unstable PS points are discarded. Only in combination allow these tests to detect all instabilities. As indicated above, this has been verified by comparison with the stable BCKK code. One can thus also assess the error introduced by discarding PS points that are wrongly classified as unstable. The parameters have been adjusted to minimize this error. For integrated cross sections, it is approximately 0.03%.

<sup>2</sup>Sample output: scale1: 10.5817 MC:  $\pm 0.0063$  ( $\pm 0.059\%$ ) scale( $\times 2$ ):  $-2.5573$  ( $-24\%$ )  $+3.6967$  ( $+35\%$ ) PDF:  $-0.2723$  ( $-2.6\%$ )  $+0.2382$  ( $+2.3\%$ ) fb, sym. scale error:  $\pm 28\%$ , sym. PDF error:  $\pm 2.4\%$ , scale2: 19.121 MC:  $\pm 0.012$  ( $\pm 0.061\%$ ) fb

<sup>3</sup>Differential distributions are smooth, even when calculating extreme cross sections like  $\sigma(p_{TV} < 1 \text{ GeV})$ .

<sup>4</sup>The PS point is assumed to be given in the rest frame of  $p_{\text{boost}}$ . The PS point is boosted to the frame in which  $p_{\text{boost}}$  is given.

process	cuts	$\sigma$ [fb], $pp$ , $\sqrt{s} = 7$ TeV, $M_H = 400$ GeV			interference	
		$ \mathcal{M}_H ^2$	$ \mathcal{M}_{\text{cont}} ^2$	$ \mathcal{M}_H + \mathcal{M}_{\text{cont}} ^2$	$R_1$	$R_2$
$gg (\rightarrow H) \rightarrow WW$	stand.	4.361(3)	6.351(4)	10.582(7)	0.9879(8)	0.970(2)
$gg (\rightarrow H) \rightarrow WW$	Higgs	2.502(2)	0.633(1)	3.007(3)	0.959(2)	0.949(2)
$gg (\rightarrow H) \rightarrow ZZ$	stand.	0.3654(4)	0.3450(4)	0.7012(8)	0.987(2)	0.975(3)
$gg (\rightarrow H) \rightarrow ZZ$	Higgs	0.2729(3)	0.01085(2)	0.2867(3)	1.010(2)	1.011(2)

**Table 1:** Cross sections in fb for  $gg (\rightarrow H) \rightarrow W^-W^+ \rightarrow l\bar{\nu}_l\bar{l}'\nu_{l'}$  and  $gg (\rightarrow H) \rightarrow ZZ \rightarrow l\bar{l}l'\bar{l}'$  in  $pp$  collisions at  $\sqrt{s} = 7$  TeV for  $M_H = 400$  GeV and a single lepton flavour combination calculated at LO. Standard cuts and Higgs search cuts are applied (see main text). Interference effects are illustrated through  $R_1 = \sigma(|\mathcal{M}_{VV}|^2)/\sigma(|\mathcal{M}_H|^2 + |\mathcal{M}_{\text{cont}}|^2)$  and  $R_2 = \sigma(|\mathcal{M}_H|^2 + 2\text{Re}(\mathcal{M}_H\mathcal{M}_{\text{cont}}^*))/\sigma(|\mathcal{M}_H|^2)$ .

### 3. Results

Parton-level cross sections for  $gg (\rightarrow H) \rightarrow W^-W^+ \rightarrow l\bar{\nu}_l\bar{l}'\nu_{l'}$  and  $gg (\rightarrow H) \rightarrow ZZ \rightarrow l\bar{l}l'\bar{l}'$  ( $l$ : charged lepton) in  $pp$  collisions at  $\sqrt{s} = 7$  TeV are presented in Table 1. Results are given for a single lepton flavour combination, e.g.  $l = e^-$ ,  $l' = \mu^-$ . Lepton masses are neglected. The input parameter set of Ref. [36], App. A, is used with NLO  $\Gamma_V$  and  $G_\mu$  scheme. For the Higgs resonance, we set  $M_H = 400$  GeV and  $\Gamma_H = 29.16$  GeV [37]. The renormalisation and factorisation scales are set to  $M_H/2$ . The PDF set MSTW2008LO with 1-loop running for  $\alpha_s(\mu^2)$  and  $\alpha_s(M_Z^2) = 0.13939$  is used. The fixed-width prescription is used for Higgs and weak boson propagators. For ZZ production and decay, the virtual photon contributions have been included.

The following experimental selection cuts are adopted [36, 38]: As  $WW$  standard cuts, we use  $p_{Tl} > 20$  GeV,  $|\eta_l| < 2.5$ ,  $p_T > 30$  GeV and  $M_{l\bar{l}'} > 12$  GeV. As  $WW$  Higgs search cuts for  $M_H = 400$  GeV, we use the  $WW$  standard cuts and in addition  $p_{Tl,\text{min}} > 25$  GeV,  $p_{Tl,\text{max}} > 90$  GeV,  $M_{l\bar{l}'} < 300$  GeV and  $\Delta\phi_{l\bar{l}'} < 175^\circ$ . As  $ZZ$  standard cuts, we use  $p_{Tl} > 20$  GeV,  $|\eta_l| < 2.5$  and  $76$  GeV  $< M_{l\bar{l}'}, M_{l'\bar{l}} < 106$  GeV. As  $ZZ$  Higgs search cuts, we use the  $ZZ$  standard cuts and in addition  $|M_{l\bar{l}l'\bar{l}'} - M_H| < \Gamma_H$ .

The significance of a Higgs or new physics observation is determined as function of the number of signal events  $S \propto \sigma(|\mathcal{M}_{\text{sig}}|^2)$  and background events  $B \propto \sum \sigma(|\mathcal{M}_{\text{bkg}}|^2)$ . When signal and background interfere the distinction becomes blurred. Here:  $|\mathcal{M}_{VV}|^2 = |\mathcal{M}_H|^2 + |\mathcal{M}_{\text{cont}}|^2 + 2\text{Re}(\mathcal{M}_H\mathcal{M}_{\text{cont}}^*)$ . One can choose to include the interference term in the signal:  $S_i \propto \sigma(|\mathcal{M}_H|^2 + 2\text{Re}(\mathcal{M}_H\mathcal{M}_{\text{cont}}^*))$ .<sup>5</sup> We assess interference effects using two measures:  $R_1 = \sigma(|\mathcal{M}_{VV}|^2)/\sigma(|\mathcal{M}_H|^2 + |\mathcal{M}_{\text{cont}}|^2)$  and  $R_2 = \sigma(|\mathcal{M}_H|^2 + 2\text{Re}(\mathcal{M}_H\mathcal{M}_{\text{cont}}^*))/\sigma(|\mathcal{M}_H|^2)$ . As shown in Table 1, at  $\sqrt{s} = 7$  TeV interference effects can be as large as 5%. At  $\sqrt{s} = 14$  TeV, interference effects can approach the 10% level: for  $WW$  production and standard cuts (Higgs search cuts) one obtains  $R_1 = 0.9680(8)$  ( $R_1 = 0.940(2)$ ) and  $R_2 = 0.932(2)$  ( $R_2 = 0.926(2)$ ), and for  $ZZ$  production and standard cuts (Higgs search cuts) one obtains  $R_1 = 0.969(2)$  ( $R_1 = 1.011(2)$ ) and  $R_2 = 0.945(3)$  ( $R_2 = 1.011(3)$ ). While the additional Higgs search cuts increase the negative interference for  $WW$  production, for  $ZZ$  production the  $|M_{l\bar{l}l'\bar{l}'} - M_H| < \Gamma_H$  cut limits the interference effect to about 1%. The latter

<sup>5</sup>In principle,  $S_i$  can be negative, and this does affect phenomenologically relevant distributions [24].

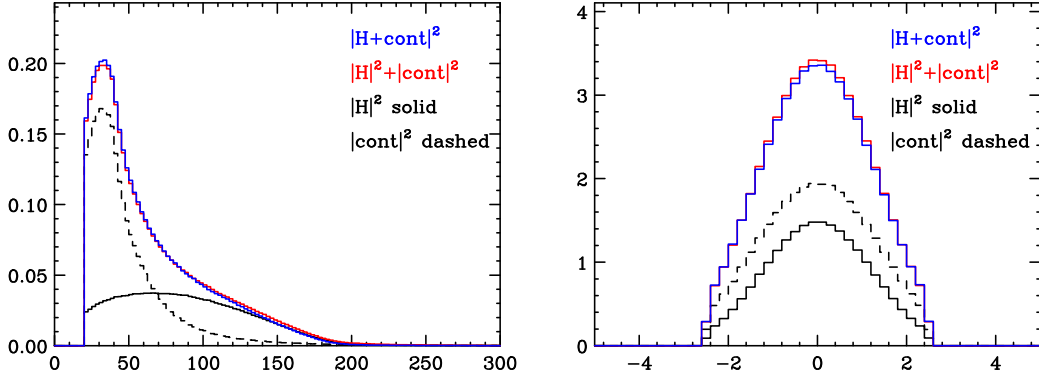


**Figure 3:** Differential cross section distributions for  $gg (\rightarrow H) \rightarrow W^-W^+ \rightarrow l\bar{\nu}_l\bar{l}'\nu_{l'}$  in  $pp$  collisions at  $\sqrt{s} = 7$  TeV for  $M_H = 400$  GeV and a single lepton flavour combination calculated at LO. The  $p_{Tl}$  [GeV] (left) and  $\eta_l$  (right) distributions are shown. Standard cuts are applied (see main text). fb is used as cross section unit.

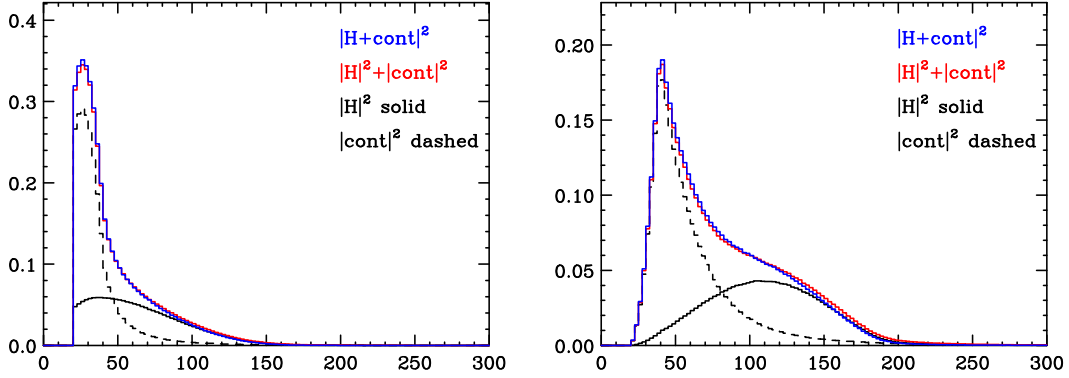


**Figure 4:**  $p_{Tl,\min}$  [GeV] (left) and  $p_{Tl,\max}$  [GeV] (right) distributions. Other details as in Fig. 3.

traces back to the fact that the interference changes sign at  $M_{l\bar{l}'\bar{\nu}} = M_H$ , as seen in Fig. 6 (left).

Differential distributions for phenomenologically relevant observables are shown in Figs. 3, 4 and 5 for  $WW$  production and in Fig. 6 for  $ZZ$  production. The distributions demonstrate that a compensation of positive and negative interference occurs for cross sections that are integrated over most of the phase space. For this reason, the more exclusive selection cuts typically used in Higgs and new physics searches can increase the size of the interference effects.

#### 4. Conclusions

$gg (\rightarrow H) \rightarrow VV$  interference effects are not suppressed and can range from 1% to about 10%. They can be enhanced by Higgs search selection cuts and should be taken into account in the LHC data analysis.

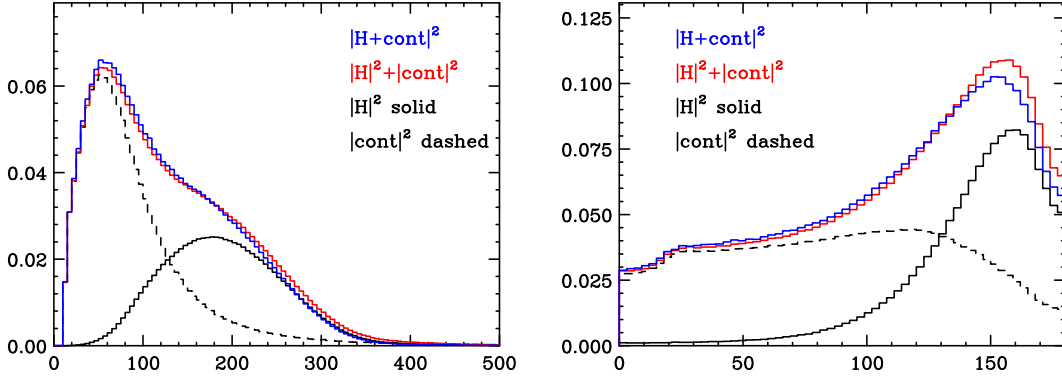


**Figure 5:**  $M_{l\bar{l}}$  [GeV] (left) and  $\Delta\phi_{l\bar{l}}$  [°] (right) distributions. Other details as in Fig. 3.

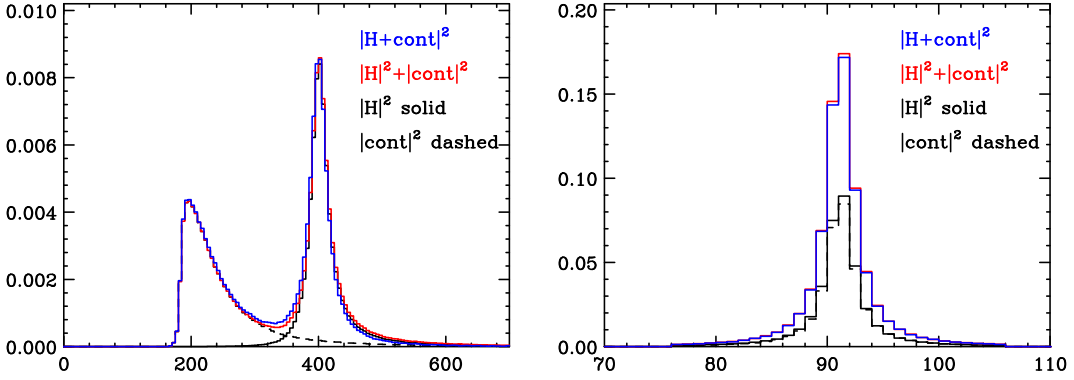


**Figure 6:** Differential cross section distributions for  $gg (\rightarrow H) \rightarrow ZZ \rightarrow l\bar{l}l'\bar{l}'$  in  $pp$  collisions at  $\sqrt{s} = 7$  TeV for  $M_H = 400$  GeV and a single lepton flavour combination calculated at LO. The  $M_{l\bar{l}l'\bar{l}'}$  [GeV] (left) and  $M_{l\bar{l}}$  [GeV] (right) distributions are shown. Standard cuts are applied (see main text). fb is used as cross section unit.

## Acknowledgments

First, I would like to thank the organisers for the invitation to speak at the RADCOR 2011 conference. Helpful discussions with A. Djouadi and M. Krämer in the initial stage of this project are gratefully acknowledged. I would also like to thank G. Heinrich for important discussions and numerical comparisons of the employed  $gg \rightarrow W^-W^+ \rightarrow l\bar{\nu}_l\bar{l}'\nu_{l'}$  and  $gg \rightarrow Z(\gamma^*)Z(\gamma^*) \rightarrow l\bar{l}l'\bar{l}'$  amplitudes with `golem-2.0` [39] generated implementations. Helpful discussions with N. De Filippis, R. K. Ellis, C. Mariotti, P. Nason, S. Pozzorini, I. Puljak, T. Riemann, R. Tanaka and D. Zeppenfeld are also gratefully acknowledged. This work was carried out as part of the research programme of the Royal Holloway and Sussex Particle Physics Theory Consortium and the NExT Institute. Financial support under the SEPnet Initiative from the Higher Education Funding Council for England and the Science and Technology Facilities Council (STFC) is gratefully acknowledged. This work was supported by STFC grant ST/J000485/1.

## References

- [1] A. Djouadi, M. Spira and P. M. Zerwas, *Production of Higgs bosons in proton colliders: QCD corrections*, Phys. Lett. B **264** (1991) 440.
- [2] S. Dawson, *Radiative corrections to Higgs boson production*, Nucl. Phys. B **359** (1991) 283.
- [3] M. Spira, A. Djouadi, D. Graudenz and P. M. Zerwas, *Higgs boson production at the LHC*, Nucl. Phys. B **453** (1995) 17 [hep-ph/9504378].
- [4] R. V. Harlander and W. B. Kilgore, *Next-to-next-to-leading order Higgs production at hadron colliders*, Phys. Rev. Lett. **88** (2002) 201801 [hep-ph/0201206].
- [5] C. Anastasiou and K. Melnikov, *Higgs boson production at hadron colliders in NNLO QCD*, Nucl. Phys. B **646** (2002) 220 [arXiv:hep-ph/0207004].
- [6] V. Ravindran, J. Smith and W. L. van Neerven, *NNLO corrections to the total cross section for Higgs boson production in hadron-hadron collisions*, Nucl. Phys. B **665** (2003) 325 [arXiv:hep-ph/0302135].
- [7] C. Anastasiou, K. Melnikov and F. Petriello, *Higgs boson production at hadron colliders: differential cross sections through next-to-next-to-leading order*, Phys. Rev. Lett. **93** (2004) 262002 [arXiv:hep-ph/0409088].
- [8] C. Anastasiou, G. Dissertori and F. Stockli, *NNLO QCD predictions for the  $H \rightarrow WW \rightarrow l\nu l\nu$  signal at the LHC*, JHEP **0709** (2007) 018 [arXiv:0707.2373 [hep-ph]].
- [9] S. Catani and M. Grazzini, *A NNLO subtraction formalism in hadron collisions and its application to Higgs boson production at the LHC*, Phys. Rev. Lett. **98** (2007) 222002 [arXiv:hep-ph/0703012].
- [10] M. Grazzini, *NNLO predictions for the Higgs boson signal in the  $H \rightarrow WW \rightarrow l\nu l\nu$  and  $H \rightarrow ZZ \rightarrow 4l$  decay channels*, JHEP **0802** (2008) 043 [arXiv:0801.3232 [hep-ph]].
- [11] C. Anastasiou, S. Buehler, F. Herzog and A. Lazopoulos, *Total cross section for Higgs boson hadroproduction with anomalous Standard Model interactions*, JHEP **1112** (2011) 058 [arXiv:1107.0683 [hep-ph]].
- [12] J. M. Campbell and R. K. Ellis, *An update on vector boson pair production at hadron colliders*, Phys. Rev. D **60** (1999) 113006 [hep-ph/9905386].
- [13] J. M. Campbell, R. K. Ellis and C. Williams, *Vector boson pair production at the LHC*, JHEP **1107** (2011) 018 [arXiv:1105.0020 [hep-ph]].
- [14] T. Melia, P. Nason, R. Rontsch and G. Zanderighi,  *$W^+W^-$ ,  $WZ$  and  $ZZ$  production in the POWHEG BOX*, JHEP **1111** (2011) 078 [arXiv:1107.5051 [hep-ph]].
- [15] D. A. Dicus, C. Kao and W. W. Repko, *Gluon production of gauge bosons*, Phys. Rev. D **36** (1987) 1570.
- [16] E. W. N. Glover and J. J. van der Bij, *Vector boson pair production via gluon fusion*, Phys. Lett. B **219** (1989) 488.
- [17] E. W. N. Glover and J. J. van der Bij, *Z-boson pair production via gluon fusion*, Nucl. Phys. B **321** (1989) 561.
- [18] C. Kao and D. A. Dicus, *Production of  $W^+W^-$  from gluon fusion*, Phys. Rev. D **43** (1991) 1555.
- [19] C. Zecher, T. Matsuura and J. J. van der Bij, *Leptonic signals from off-shell Z-boson pairs at hadron colliders*, Z. Phys. C **64** (1994) 219 [hep-ph/9404295].

- [20] T. Binoth, M. Ciccolini, N. Kauer and M. Kramer, *Gluon-induced  $WW$  background to Higgs boson searches at the LHC*, JHEP **0503** (2005) 065 [hep-ph/0503094].
- [21] M. Duhrssen, K. Jakobs, J. J. van der Bij and P. Marquard, *The process  $gg \rightarrow WW$  as a background to the Higgs signal at the LHC*, JHEP **0505** (2005) 064 [hep-ph/0504006].
- [22] T. Binoth, M. Ciccolini, N. Kauer and M. Kramer, *Gluon-induced  $W$ -boson pair production at the LHC*, JHEP **0612** (2006) 046 [hep-ph/0611170].
- [23] T. Binoth, N. Kauer and P. Mertsch, *Gluon-induced QCD corrections to  $pp \rightarrow ZZ \rightarrow \bar{l}l'l'$* , in proceedings of XVI Int. Workshop on Deep-Inelastic Scattering and Related Topics, London, England, April 2008, arXiv:0807.0024 [hep-ph].
- [24] J. M. Campbell, R. K. Ellis and C. Williams, *Gluon-gluon contributions to  $W^+W^-$  production and Higgs interference effects*, JHEP **1110** (2011) 005 [arXiv:1107.5569 [hep-ph]].
- [25] R. Frederix, S. Frixione, V. Hirschi, F. Maltoni, R. Pittau and P. Torrielli, *Four-lepton production at hadron colliders: aMC@NLO predictions with theoretical uncertainties*, arXiv:1110.4738 [hep-ph].
- [26] M. H. Seymour, *The Higgs boson line shape and perturbative unitarity*, Phys. Lett. B **354** (1995) 409 [hep-ph/9505211].
- [27] L. J. Dixon and M. S. Siu, *Resonance-continuum interference in the diphoton Higgs signal at the LHC*, Phys. Rev. Lett. **90** (2003) 252001 [hep-ph/0302233].
- [28] L. J. Dixon and Y. Sofianatos, *Resonance-continuum interference in light Higgs boson production at a photon collider*, Phys. Rev. D **79** (2009) 033002 [arXiv:0812.3712 [hep-ph]].
- [29] D. Boer, W. J. den Dunnen, C. Pisano, M. Schlegel and W. Vogelsang, *Linearly polarized gluons and the Higgs transverse momentum distribution*, Phys. Rev. Lett. **108** (2012) 032002 [arXiv:1109.1444 [hep-ph]].
- [30] U. Baur and E. W. N. Glover, *Observability of a heavy Higgs boson at hadron supercolliders*, Phys. Rev. D **44** (1991) 99.
- [31] J. Bagger, V. D. Barger, K. Cheung, J. F. Gunion, T. Han, G. A. Ladinsky, R. Rosenfeld and C. P. Yuan, *The strongly interacting  $WW$  system: gold plated modes*, Phys. Rev. D **49** (1994) 1246 [hep-ph/9306256].
- [32] K. Iordanidis and D. Zeppenfeld, *Searching for a heavy Higgs boson via the  $H \rightarrow lvjj$  mode at the CERN LHC*, Phys. Rev. D **57** (1998) 3072 [hep-ph/9709506].
- [33] S. Goria, G. Passarino and D. Rosco, *The Higgs boson lineshape*, arXiv:1112.5517 [hep-ph].
- [34] T. Hahn and M. Perez-Victoria, *Automatized one-loop calculations in four and  $D$  dimensions*, Comput. Phys. Commun. **118** (1999) 153 [arXiv:hep-ph/9807565].
- [35] T. Hahn, *Generating Feynman diagrams and amplitudes with FeynArts 3*, Comput. Phys. Commun. **140** (2001) 418 [arXiv:hep-ph/0012260].
- [36] S. Dittmaier *et al.* [LHC Higgs Cross Section Working Group Collaboration], *Handbook of LHC Higgs cross sections: 1. Inclusive observables*, arXiv:1101.0593 [hep-ph].
- [37] A. Djouadi, J. Kalinowski and M. Spira, *HDECAY: a program for Higgs boson decays in the Standard Model and its supersymmetric extension*, Comput. Phys. Commun. **108** (1998) 56 [hep-ph/9704448].
- [38] S. Chatrchyan *et al.* [CMS Collaboration], *Measurement of  $W^+W^-$  production and search for the Higgs boson in  $pp$  collisions at  $\sqrt{s} = 7$  TeV*, Phys. Lett. B **699** (2011) 25 [arXiv:1102.5429 [hep-ex]].
- [39] G. Cullen, N. Greiner, G. Heinrich, G. Luisoni, P. Mastrolia, G. Ossola, T. Reiter and F. Tramontano, *Automated one-loop calculations with GoSam*, arXiv:1111.2034 [hep-ph].